Realisation of gyrators using operational amplifiers, and their use in *RC*-active-network synthesis

A. Antoniou, B.Sc.(Eng.), Ph.D.

Abstract

The realisation of negative-impedance convertors (n.i.c.s) and invertors (n.i.i.s) using the bridge-type circuit is briefly surveyed. An equivalence relating the nullor to infinite-gain controlled sources is first proved, and is then used for the derivation of nullator–norator equivalent circuits for n.i.c.s and n.i.i.s. Some properties of networks containing singular elements, which are used in the realisation of gyrators, are investigated. Nullator–norator equivalent circuits for gyrators are derived by using the n.i.c.s and n.i.i.s. They are converted into physical networks by using the proved equivalence. Gyrator circuits are obtained by replacing nullors by operational amplifiers. A stability analysis of the gyrator circuits is produced and a relevant theorem concerning passivity is proved. The feasible Q factors and the accuracy of the gyrator circuits are indicated by some experimental results. A generalised-impedance convertor (g.i.c.) is defined by generalising the n.i.c. theory, and it is shown that the gyrator circuits described can be used as g.i.c.s. The application of the gyrator and g.i.c. circuits in the synthesis of *RC*-active networks is considered. Finally, a highpass filter using gyrators and a bandpass filter using g.i.c.s are designed, and the experimental results are given.

List of principal symbols

A, B, C, D, K = positive constants
$[A]$ = chain matrix $(a_{11}, a_{12}, a_{21}, a_{22})$
$D(s)$ = denominator polynomial in s
$f(s)$ = impedance-conversion function of g.i.c.
G = voltage gain of a voltage-controlled voltage source
G_o = differential gain of an operational amplifier at d.c.
G_1, G_2 = differential gains of operational amplifiers
H = current gain of a current-controlled current source
$H_a(s), H_b(s)$ = positive real functions
k = gyration constant
k_m = measured gyration constant
k_{nom} = nominal gyration constant
k_1 = conversion factor of negative-impedance convertor
k_2 = inversion factor of negative-impedance invertor
$N(s)$ = numerator polynomial in s
s = complex frequency variable $(= \sigma + j\omega)$
$[Y]$ = Ymatrix
$[Z]$ = Zmatrix
$Z_i(s)$ = input impedance
$Z_L(s)$ = load impedance
$-\omega_c$ = dominant pole of amplifier gain
ω_m = maximum frequency at which the dominant-pole approximation for the amplifier gain is valid

1 Introduction

At present, miniature inductors have small Q factors,[1] the feasible inductance range is limited, and they are not compatible with either integrated-circuit or thin-film technology. In an effort to produce frequency-selective networks without inductors, several types of active elements have been used, such as controlled sources, operational amplifiers and negative-impedance convertors (n.i.c.s). [An n.i.c. is an active 2-port network which has an input impedance of $-k_1 Z_L$ when terminated by Z_L $(k_1 > 0)$.] A variety of synthesis procedures, using the above active elements have been proposed.[2] It has been established that, in general, these methods are satisfactory for the realisation of second-order transfer functions with Q factors in the range 0–30. Although second-order transfer functions with higher Q factors can be realised in theory, on considering the sensitivity of the response function to element variations, it is found that very stable and close-tolerance elements are needed. Consequently, the resulting realisations become impracticable.

An element which promises to reduce drastically the sensitivity problem is the gyrator.[3] It is a 2-port network with an input impedance k/Z_L when terminated by Z_L $(k > 0)$. A gyrator simulates an inductance when terminated by a capacitance, and so passive RLC networks can be synthetised using only resistors, capacitors and gyrators. The expected reduction in the sensitivity is due to the relative insensitivity of the passive networks.[4]

Several gyrator circuits have been published.[5–11] The majority of these are realisations of an ideal circuit given by Sharpe,[12] where two voltage-controlled current sources (v.c.c.s.s), one with positive and the other with negative gain, are connected in parallel and back to back. Some of these can be produced as integrated circuits.[7–9] A few realisations[13–14] consist of electronic circuits which exhibit gyrator properties. However, the simulated inductance has a large series resistance which is cancelled by using a negative resistance.

Integrated-circuit operational amplifiers are readily available in a variety of specifications, and are ideal as 'building blocks' for the realisation of gyrators. This paper investigates the realisation of gyrators using operational amplifiers. Their application to the synthesis of RC-active networks is also considered.

2 Realisation of negative-impedance convertors and invertors

The realisation of n.i.c.s and negative-impedance invertors (n.i.i.s) is now considered, as they will be used in the realisation of gyrators. An n.i.i. is an active 2-port network which has an input impedance of $-k_2/Z_L$ when terminated by Z_L $(k_2 > 0)$.

There are two types of n.i.c., the voltage-inversion type (v.n.i.c.) which has a chain matrix as follows:

$$\begin{bmatrix} V_1 \\ I_1 \end{bmatrix} = [A]_{v.n.i.c.} \begin{bmatrix} V_2 \\ -I_2 \end{bmatrix} \quad \ldots\ldots\ldots \quad (1)$$

where $[A]_{v.n.i.c.} = \begin{bmatrix} -\dfrac{R_1}{R_2} & 0 \\ 0 & 1 \end{bmatrix}$

and the current-inversion type (c.n.i.c.) which has

$$[A]_{c.n.i.c.} = \begin{bmatrix} 1 & 0 \\ 0 & -\dfrac{R_2}{R_1} \end{bmatrix} \quad \ldots\ldots\ldots \quad (2)$$

where $(R_1/R_2) = k_1$

Paper 5952 E, first received 21st January and in revised form 18th June 1969
Dr. Antoniou was formerly with the British Post Office Research Department, Dollis Hill, London NW2, England, and is now with the Research & Development Laboratories, Northern Electric Co., P.O. Box 3511, Station C, Ottawa, Ont., Canada

The chain matrix of an n.i.i. is

$$[A]_{n.i.i.} = \begin{bmatrix} 0 & \pm R_2 \\ \mp \dfrac{1}{R_1} & 0 \end{bmatrix} \quad \ldots\ldots\ldots \quad (3)$$

where $R_1 R_2 = k_2$.

Larky[15] and Lundry[16] have used the bridge-type circuit,

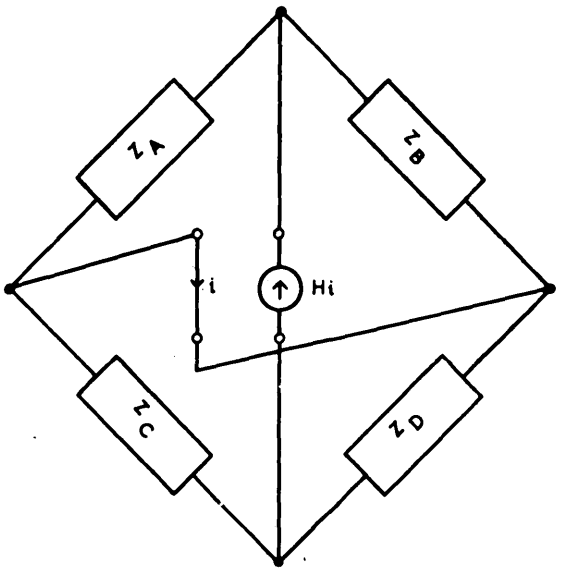

Fig. 1
Bridge-type circuit used for the realisation of n.i.c.s and n.i.i.s

shown in Fig. 1, to derive c.n.i.c.s, v.n.i.c.s and n.i.i.s. These circuits can be derived as indicated in Table 1.

Table 1

DERIVATION OF N.I.C.S AND N.I.I.S

Type of circuit	Z_A	Z_B	Z_C	Z_D
c.n.i.c. . . .	R_1	R_2	∞	∞
v.n.i.c. . . .	∞	∞	R_1	R_2
n.i.i.	R_1	∞	∞	R_2

3 Singular elements

In this Section, an equivalence relating the singular elements to controlled sources is proved. This will be used in the derivation of n.i.c.s, n.i.i.s and gyrators using operational amplifiers.

The singular elements described by Carlin and Youla[17] are the nullator and norator. The nullator shown in Fig. 2*a*, is a 1-port which will neither sustain a voltage nor pass a current (i.e. $V = I = 0$). On the other hand, the norator in Fig. 2*b*, is a 1-port which will sustain an arbitrary voltage and pass an arbitrary current which are independent of each other. A 2-port consisting of a nullator as port 1 and a norator as port 2, as shown in Fig. 2*c*, has been defined as a nullor.[18] Martinelli[19] has shown that an ideal transistor is equivalent to a nullor. Butler[20] and Davies[21] have also demonstrated, without a general proof, that an infinite-gain voltage-controlled voltage source (v.c.v.s.) is also equivalent to a nullor. A proof of this equivalence is now provided. In addition, the three remaining types of infinite-gain controlled source are shown to be equivalent to nullors.

Consider a v.c.v.s. embedded in a general 3-port network N, as shown in Fig. 2*d*. It is assumed that N has a finite Ymatrix

$$[I] = [Y][V] \quad \ldots\ldots\ldots\ldots \quad (4)$$

or a finite Zmatrix

$$[V] = [Z][I] \quad \ldots\ldots\ldots\ldots \quad (5)$$

From the definition of a v.c.v.s., $I_3 = 0$ and $V_2 = GV_3$. Hence, from eqn. 4,

$$V_3 = \frac{(-Y_{31})V_1}{Y_{33} + GY_{32}} \quad \ldots\ldots\ldots\ldots \quad (6)$$

It is assumed that a transmission path exists between ports 2 and 3 so that $Y_{32} \neq 0$. Since the Ymatrix is finite, as $G \to +\infty$ (or $G \to -\infty$), $V_3 \to 0$. Eqn. 4 gives

$$V_2 = \frac{-Y_{31}}{Y_{32}} V_1 \quad \ldots\ldots\ldots\ldots \quad (7)$$

$$I_2 = \left(Y_{21} - \frac{Y_{22}Y_{31}}{Y_{32}}\right) V_1 \quad \ldots\ldots\ldots \quad (8)$$

We wish to represent the v.c.v.s. by two 1-ports, as shown in

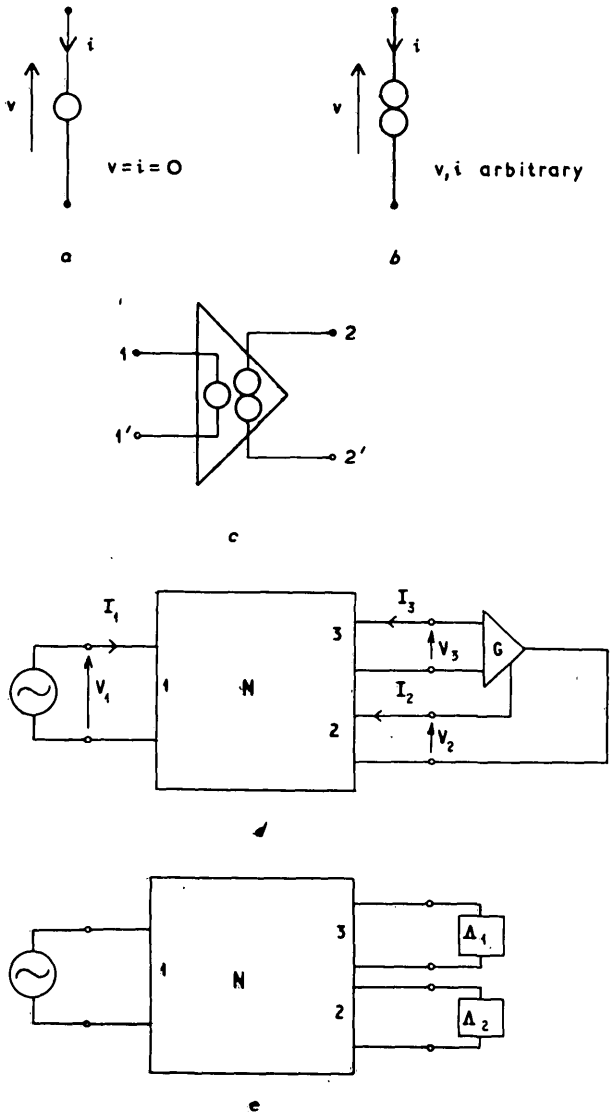

Fig. 2
Singular elements
a Nullator
b Norator
c Nullor
d Infinite-gain controlled source embedded in a general 3-port network
e Replacement of controlled source by two 1-ports

Fig. 2*e*. Since $V_3 = I_3 = 0$, Λ_1 is a nullator. Eqns. 7 and 8 show that V_2 and I_2 can be varied arbitrarily and independently by modifying the network N. Hence Λ_2 is a norator. On using the Zmatrix and replacing the voltage source V_1 by a current source I_1, the same result can be established.

The equivalence can be extended to an infinite-gain current-controlled current source (c.c.c.s.). By replacing the v.c.v.s. by a c.c.c.s. in Fig. 2*d*, $V_3 = 0$ and $I_2 = HI_3$ (H is the current gain). If the voltage source V_1 is replaced by a current source I_1, from eqn. 5,

$$I_3 = \frac{(-Z_{31})I_1}{Z_{33} + HZ_{32}} \quad \ldots\ldots\ldots\ldots \quad (9)$$

It is assumed that $Z_{32} \neq 0$ so that when $H \to +\infty$ (or $H \to -\infty$) $I_3 \to 0$. Therefore, Λ_1 is a nullator and Λ_2 can be shown to be a norator by deriving dual relations to those given in eqns. 7 and 8. This result can also be established by using the Ymatrix in Fig. 2*d*.

Similarly, an infinite-gain voltage-controlled current source

(v.c.c.s.) and an infinite-gain current-controlled voltage source (c.c.v.s.) can be shown to be equivalent to nullors.

Network N in Fig. 2*d* may contain n infinite-gain controlled sources. By treating the input nodes of the controlled source r ($1 \leqslant r \leqslant n$) as port 3 and its output nodes as port 2, if $Y_{32}^r \neq 0$ (or $Z_{32}^r \neq 0$) for all r, all controlled sources can be

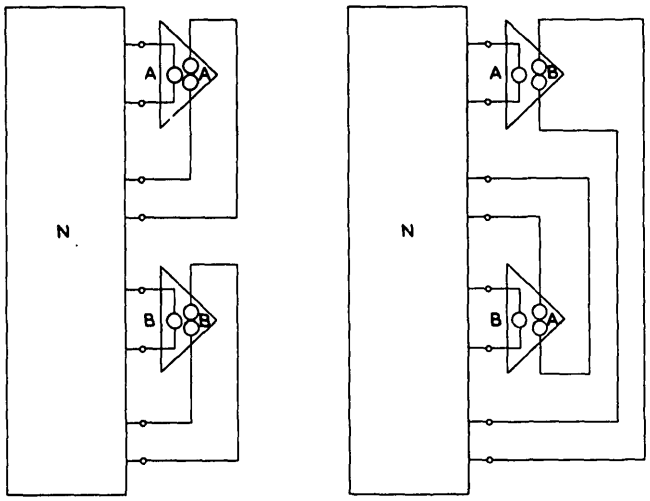

Fig. 3

Two alternative nullor equivalent networks obtained from a single nullator–norator equivalent network

replaced by nullors and a nullor equivalent network will result. The nullors can be split into nullators and norators to yield a nullator–norator equivalent network.

In reverse, a nullator–norator equivalent network containing n nullators and n norators yields $n!$ nullor equivalent networks, since nullators and norators can be paired into nullors in an arbitrary manner. For example, a nullator–norator equivalent network containing two nullators and two norators yields two nullor equivalent networks as shown in Fig. 3, since nullator A can be paired with norator A or B and nullator B with norator B or A.

Each nullor equivalent network is now considered as a 3-port network similar to that in Fig. 2*e*, where the nullor r is connected between ports 3 and 2 (nullator at port 3). If $Y_{32}^r \neq 0$ (or $Z_{32}^r \neq 0$) for $1 \leqslant r \leqslant n$, each nullor corresponds to an infinite-gain controlled source. Consequently, a network containing n nullators and n norators corresponds to $n!$ networks containing infinite-gain controlled sources.

Although the nullator (or norator) is not admissible as an idealisation of a physical network,[21-22] the nullor, like an infinite-gain controlled source, is admissible. The equivalence established is valid whether $G \to +\infty$ or $G \to -\infty$ and so, in practice, a nullor can be replaced by a high-gain differential controlled source in two ways, as shown in Fig. 4. The non-inverting-input terminal of the controlled source can be connected to a node P, and the inverting-input terminal to a node Q (Fig. 4*b*) or vice versa (Fig. 4*c*). Thus a nullor equivalent network containing two nullors corresponds to four physical networks, since either high-gain controlled source can be connected in two ways. In general, a nullor equivalent network containing n nullors corresponds to 2^n physical networks.

By using the equivalence between a nullor and an infinite-gain c.c.c.s., nullator–norator equivalent circuits for n.i.c.s and n.i.i.s can be obtained from Fig. 1, as shown in Fig. 5. The n.i.c. circuits were originally obtained by Braun[23] by replacing ideal transistors, instead of infinite-gain c.c.c.s.s, by nullors. The nullator–norator equivalent circuits can now be used to derive three more sets of n.i.c.s and n.i.i.s by replacing the nullors by v.c.v.s.s (this will yield the c.n.i.c. of Morse[24] and the n.i.i. of Reference 25), v.c.c.s.s and c.c.v.s.s.

The n.i.c. circuits of Fig. 5 are completely symmetrical about a vertical axis, so that port 1 cannot be distinguished from port 2. However, in practice, n.i.c. circuits have different stability properties at each port. For example, Brownlie[26] has shown that a d.c.-coupled n.i.c. is open-circuit unstable at one port and short-circuit unstable at the other. Therefore, singular elements do not convey any stability information. Stability properties can only be investigated after the replacement of singular elements by physical ones.

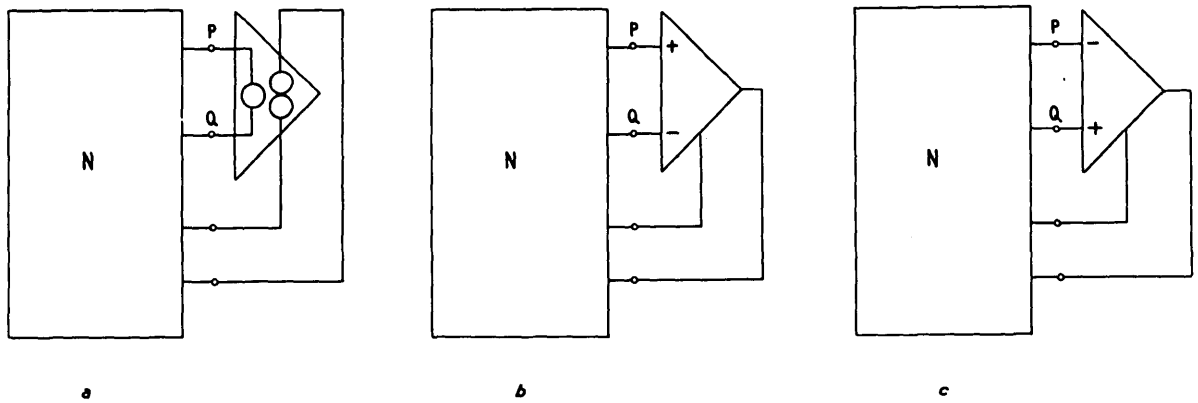

Fig. 4

Replacement of nullors by physical networks

a Circuit containing one nullor *b* and *c* Two alternative physical circuits

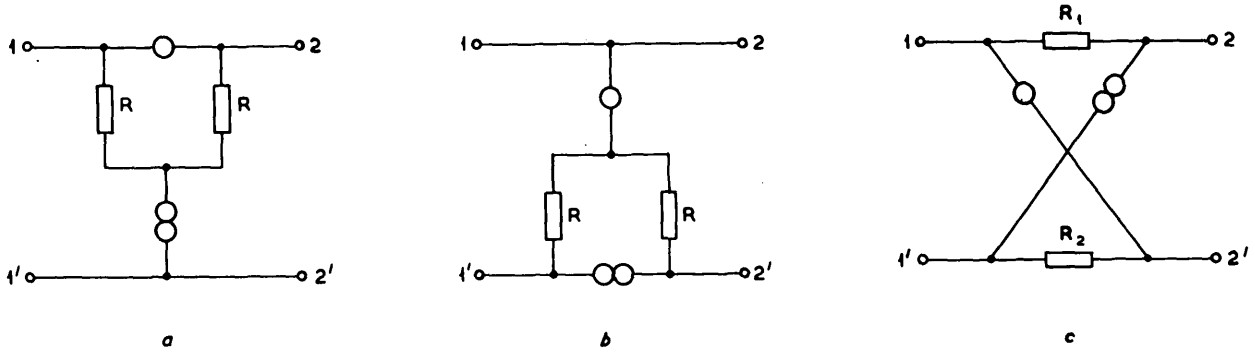

Fig. 5

Nullator–norator equivalent circuits for n.i.c.s and n.i.i.s

a C.N.I.C. *b* V.N.I.C. *c* N.I.I.

4 Realisation of gyrators

Gyrators will be realised by using n.i.c.s and n.i.i.s. The following methods are used:

(*a*) replacing a positive by a negative resistance in an n.i.i.[25]
(*b*) cascading n.i.c.s and n.i.i.s[25]
(*c*) using the theory of singular elements, alternative gyrators are derived from those obtained in (*a*) and (*b*).[27]

The chain matrix of a gyrator is

$$[A]_{gyr} = \begin{bmatrix} 0 & \pm R_2 \\ \pm \frac{1}{R_1} & 0 \end{bmatrix} \quad \ldots\ldots\ldots \quad (10)$$

where $R_1 R_2 = k$ and k is referred to as the gyration constant.

On comparing eqns. 3 and 10 it is seen that if R_2 (or R_1) of the n.i.i. is replaced by $-R_2$ (or $-R_1$), the n.i.i. becomes a gyrator. A negative resistance can be obtained by using an n.i.c. terminated by a positive resistance, as shown in Fig. 6. This is used to replace R_2 in the n.i.i. Owing to the asymmetry of the negative-resistance circuit about a horizontal axis, two connections are possible; the terminals 1 and 1′ of the negative resistance can be connected to terminals 2′ and 1′ of the n.i.i. respectively, as shown in Fig. 7*a*, or the terminals 1′ and 1 of the negative resistance can be connected to terminals 2′ and 1′ of the n.i.i respectively, as shown in Fig. 7*b*. The sign of R_1 can be changed instead of that of R_2. However, owing to the symmetry of the n.i.i. nullator–norator equivalent circuit about a horizontal axis, the same circuits result.

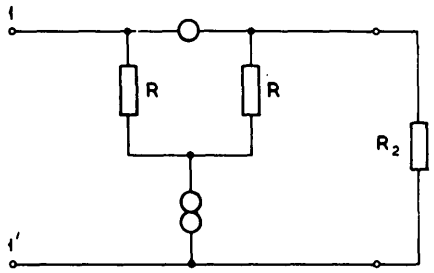

Fig. 6
Realisation of negative resistance

The chain matrix of a gyrator can be expressed as a product of matrices:

$$[A]_{gyr} = \begin{bmatrix} 0 & \pm R_2 \\ \pm \frac{1}{R_1} & 0 \end{bmatrix} = \begin{bmatrix} 1 & 0 \\ 0 & -1 \end{bmatrix} \begin{bmatrix} 0 & \pm R_2 \\ \mp \frac{1}{R_1} & 0 \end{bmatrix}$$
$$= [A]_{c.n.i.c.} \times [A]_{n.i.i.} \quad \ldots\ldots\ldots \quad (11)$$

Similarly

$$\left.\begin{aligned} [A]_{gyr} &= [A]_{n.i.i.} \times [A]_{c.n.i.c.} \\ &= [A]_{v.n.i.c.} \times [A]_{n.i.i.} \\ &= [A]_{n.i.i.} \times [A]_{v.n.i.c.} \end{aligned}\right\} \quad \ldots\ldots\ldots \quad (12)$$

Thus gyrators can be obtained by cascading n.i.c.s and n.i.i.s. Four distinct cascade circuits can be obtained as follows:

(i) cascading a c.n.i.c. and an n.i.i. so that terminals 2 and 2′ of the c.n.i.c. are connected to terminals 1 and 1′ of the n.i.i. respectively (Fig. 8*a*)
(ii) cascading an n.i.i. and a c.n.i.c. so that terminals 2 and 2′

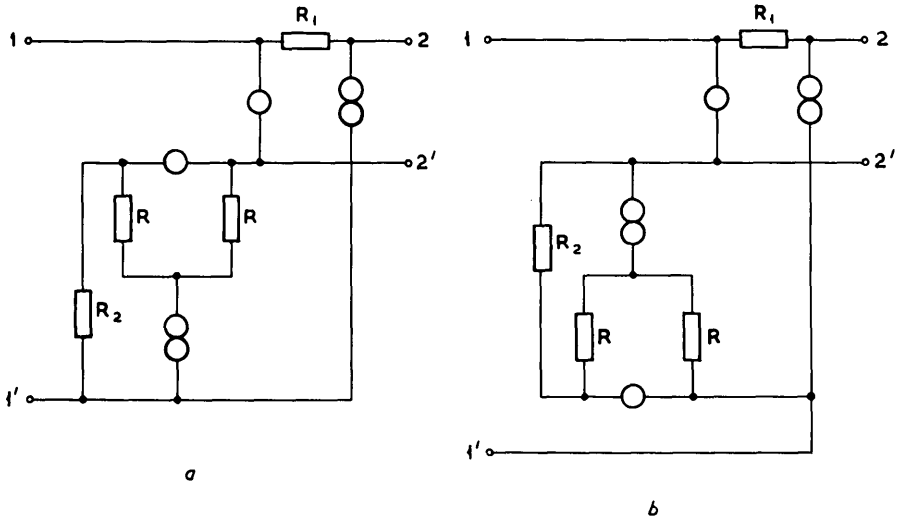

Fig. 7
Gyrators realised by replacing a positive by a negative resistance in an n.i.i.
a Nullors can be replaced by operational amplifiers
b Nullors can be replaced by transistors

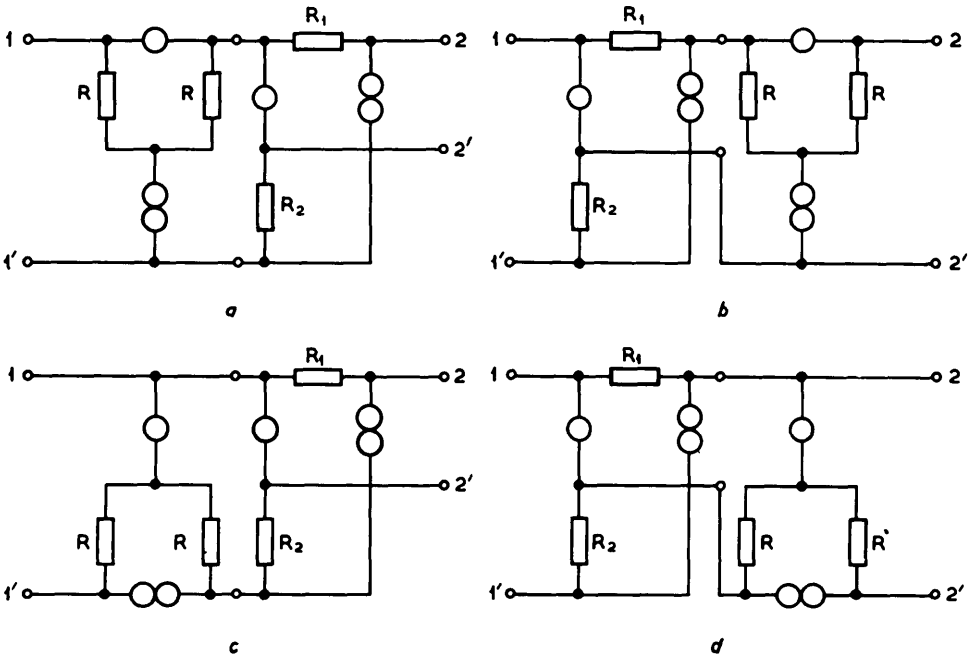

Fig. 8
Gyrators realised by cascading n.i.c.s and n.i.i.s
a Nullors can be replaced by operational amplifiers
b and *d* Nullors can be replaced by transistors

Table 2

Z PARAMETERS OF GYRATOR CIRCUITS

	Gyrator 1	Gyrator 2	Gyrator 3	Gyrator 4
Z_{11}	$\frac{-R_1}{G_1 - 1}$	$\frac{RR_1(1 + G_2) + R^2(1 - G_1)}{D_1}$	$\frac{R_1(G_1 + 1)(R + R_2)}{D_2}$	$\frac{RR_1(G_2 + 1) + R^2(G_1 + 1)}{D_3}$
Z_{12}	$\frac{k_1G_1R_2}{G_1 - 1}$	$\frac{-R_2RG_1G_2}{D_1}$	$\frac{RG_2\{R + R_2(G_1 + 1)\}}{D_2}$	$\frac{-G_2R_2\{R_1 + R(G_1 + 1)\}}{D_3}$
Z_{21}	$\frac{-G_1R_1}{G_1 - 1}$	$\frac{RR_1G_1G_2}{D_1}$	$\frac{-R_1G_1\{R_2 + R(G_2 + 1)\}}{D_2}$	$\frac{G_1R\{R + R_1(G_2 + 1)\}}{D_3}$
Z_{22}	$\frac{k_1R_2}{G_1 - 1}$	$\frac{R_1R_2(1 + G_1) + RR_2(1 - G_2)}{D_1}$	$\frac{R(G_2 + 1)(R + R_2)}{D_2}$	$\frac{R_1R_2(G_2 + 1) + RR_2(G_1 + 1)}{D_3}$

$k_1 = \frac{G_2 + (R_2 + R)/R_2}{G_2 - (R_2 + R)/R}$

$D_1 = R(G_1 - 1)(G_2 - 1) + R_1$

$D_2 = G_1G_2R + (G_1 + 1)(R + R_2)$

$D_3 = G_1G_2R + R(G_1 + 1) + R_1(G_2 + 1)$

of the n.i.i. are connected to terminals 1 and 1′ of the c.n.i.c. respectively (Fig. 8*b*)

(iii) cascading a v.n.i.c. and an n.i.i. so that terminals 2 and 2′ of the v.n.i.c. are connected to terminals 1 and 1′ of the n.i.i. respectively (Fig. 8*c*)

(iv) cascading an n.i.i. and a v.n.i.c. so that terminals 2 and 2′ of the n.i.i. are connected to terminals 1 and 1′ of the v.n.i.c. respectively (Fig. 8*d*).

It will be shown in the following Section that only the circuits in Figs. 7*a* and 8*a* can be realised by using operational amplifiers. However, the remaining circuits are also useful. It is seen that nullators and norators in Figs. 7*b* and 8*d* occur in joined pairs and hence nullors can be replaced by transistors.[19]

5 Gyrator circuits using operational amplifiers

Operational amplifiers are high-gain v.c.v.s.s and, in practice, one of their output terminals is permanently earthed. A practical gyrator circuit must have one terminal of at least one of its ports earthed. Thus one terminal of the gyrator input port and one terminal of each norator, in the nullator–norator equivalent circuit, must share a single node. Figs. 7 and 8 show that only two circuits have this property, namely those in Figs. 7*a* and 8*a*.

Each of the two nullator–norator equivalent circuits yields two distinct nullor equivalent circuits, as shown in Section 3. In turn, each nullor equivalent circuit yields four physical circuits, depending on the connections of the differential input terminals of the operational amplifiers. The only useful circuits are shown in Fig. 9. For convenience, these will be referred to as gyrator circuits 1, 2, 3 and 4. The remaining circuits have been found to be either unstable or of no practical significance. (The circuits obtained from those in Figs. 9*a* and *b* by reversing the differential input terminals of both amplifiers, can be used to convert an inductance into a capacitance or a large resistance into a small resistance).

If it is assumed that the operational amplifiers have infinite

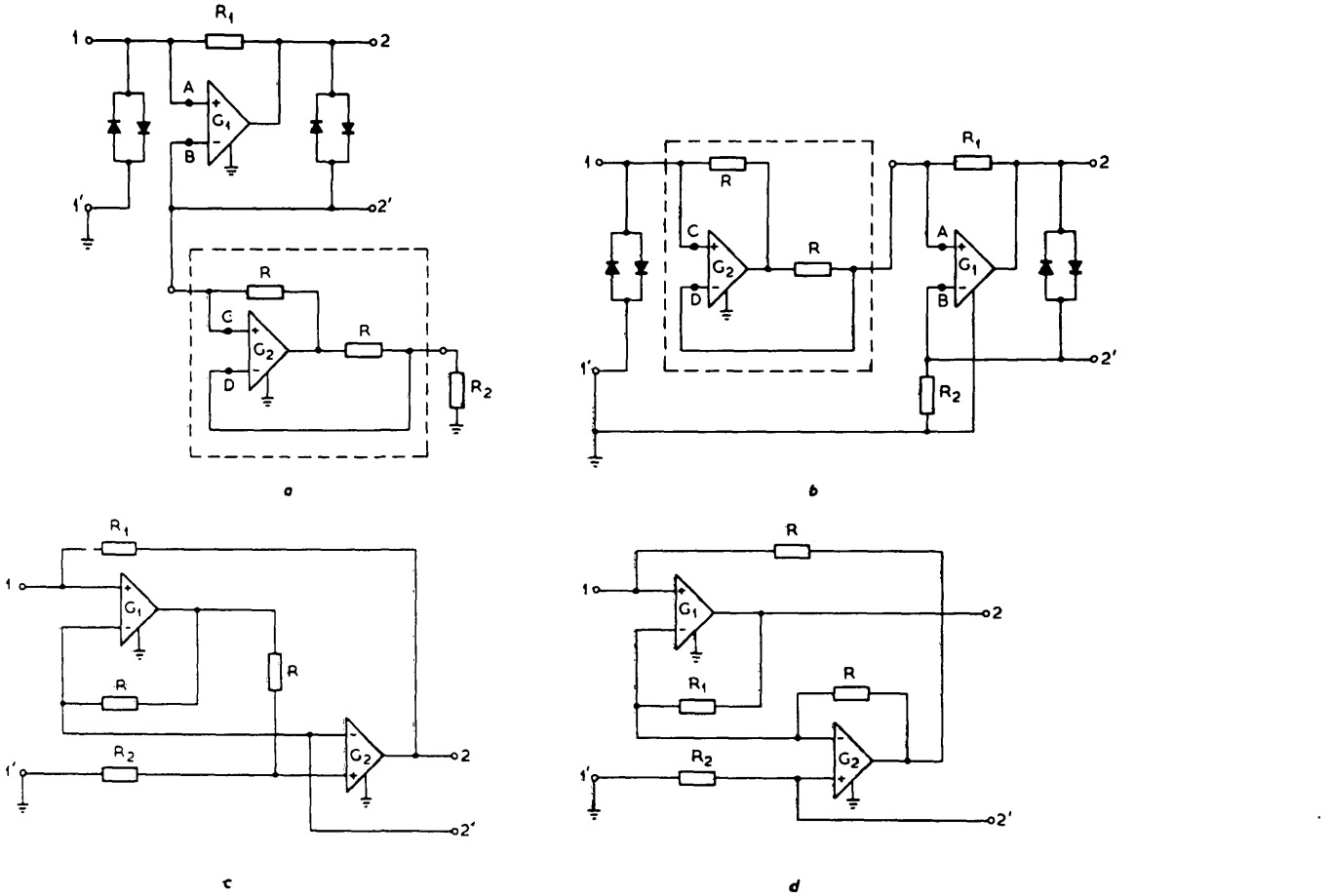

Fig. 9

Gyrator circuits using operational amplifiers

a Circuit obtained by replacing a positive by a negative resistance
b Circuit obtained by cascading a c.n.i.c. and an n.i.i.
c and *d* Alternative circuits obtained by using the theory of singular elements

input impedance, zero output impedance and finite differential gain G, analysis gives the Z parameters summarised in Table 2. In the analysis, the diodes whose action will be explained in Section 6 are assumed to have infinite resistance in both the forward and reverse directions. In practice, the diodes have large resistances in both directions for only small bias voltages, and, consequently, their use limits the voltage-handling capacity of the gyrator circuit.

6 Stability theory

The circuits shown in Fig. 9 behave as gyrators if, and only if, $|G_1|$ and $|G_2| \gg 1$. In practice, the amplifier gains can assume values in the range $0 \leqslant |G_1|$ (or $|G_2|) \leqslant |G_{max}|$ where $|G_{max}| < \infty$, since these rise from zero just after activation (switching on the direct supply voltage). It will be shown that circuits 1 and 2 can attain low-frequency unstable modes for some attainable pairs of amplifier gains. Circuits 3 and 4, however, are shown to be free from low-frequency unstable modes.

Consider a gyrator circuit with capacitances C_1 and C_2 connected across ports 1 and 2 respectively. The natural frequencies are the zeros of the circuit determinant

$$\Delta Z = \left(Z_{11} + \frac{1}{sC_1}\right)\left(Z_{22} + \frac{1}{sC_2}\right) - Z_{12}Z_{21} \quad . \quad (13)$$

The differential open-loop gain of a frequency-compensated operational amplifier, in a bounded frequency range $0 \leqslant \omega \leqslant \omega_m$, is

$$G = \frac{G_o\omega_c}{s + \omega_c} \quad . \quad . \quad . \quad . \quad . \quad . \quad (14)$$

where G_o and $-\omega_c$ are the d.c. gain and the dominant pole respectively (ω_c is a positive constant). The region $|s| \ll \omega_c$ in the s plane is of interest, and G_1 and G_2 in the Z parameters can be assumed to be real. From eqn. 13 the natural frequencies can be calculated for a series of pairs of amplifier gains in the range $0 \leqslant G_1$(or $G_2) \leqslant G_{max}$ where $G_2 = KG_1$ (K is a positive constant). For $G_1 = G_2 = 0$ a passive RC network with natural frequencies on the negative real axis of the s plane exists. When G_1 and $G_2 \gg 1$, one of the capacitances is converted to an inductance and an LC resonant circuit results; the natural frequencies are complex conjugate and lie adjacent to the j axis. Such results have been obtained for gyrator circuits 1–4, and they can be represented by root-locus diagrams as shown in Table 3.

Table 3

ROOT-LOCUS DIAGRAMS

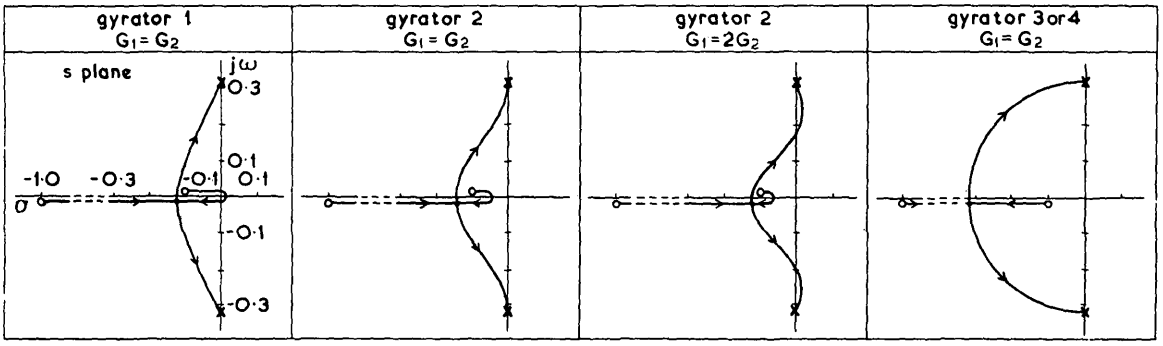

$C_1 = 1$ F, $C_2 = 10$ F, $R = 1\,\Omega$, $G_{max} = 10^5$
ω is in rad/s

The first column shows that gyrator circuit 1 attains a zero-frequency (d.c.) unstable mode. Gyrator circuit 2 attains a low-frequency unstable mode in some cases, for example when $G_1 = 2G_2$ and $C_2 = 10C_1$. In effect, circuits 1 and 2 are conditionally stable in a sense similar to that of Bode,[28] and sometimes they become unstable.

In practice, an unstable mode may be attained while the amplifier gains are rising from zero just after activation. The oscillation amplitude during the unstable mode can rise sufficiently to saturate the amplifiers. The effective amplifier gains will cease to rise owing to the nonlinearity of the dynamic characteristics of the amplifiers, and consequently, the circuit may lock in an unstable mode. Such behaviour has been observed in practice.

Circuits 1 and 2 can be prevented from locking in an unstable mode by placing diodes across each port, as shown in Fig. 9. The amplitude of any oscillation is now limited to a low level, the amplifiers are prevented from saturating, and the effective gains can rise to their final value. However, the diodes do reduce the voltage-handling capacity of the circuit.

A 2-port satisfying the Llewellyn stability criterion[29]

$$\left.\begin{aligned} &\mathrm{Re}\, Z_{11},\ \mathrm{Re}\, Z_{22} \geqslant 0 \\ &2\mathrm{Re}\, Z_{11}\, \mathrm{Re}\, Z_{22} \geqslant |Z_{12}Z_{21}| + \mathrm{Re}\, Z_{12}Z_{21} \end{aligned}\right\} \quad . \quad . \quad (15)$$

is absolutely stable (i.e. is stable for all passive terminations). At complex frequencies in the region $|s| \ll \omega_c$, G_1 and G_2 can be assumed to be real. For circuits 3 and 4, it follows from the Z parameters given in Table 2 that,

$$|Z_{12}Z_{21}| = -\mathrm{Re}\, Z_{12}Z_{21} \quad . \quad . \quad . \quad . \quad . \quad . \quad . \quad (16)$$

for all attainable values of G_1 and G_2 [i.e. $0 \leqslant G_1$(or $G_2) \leqslant G_{max}$ where $G_{max} < \infty$]. Eqns. 15 and 16 give

$$\mathrm{Re}\, Z_{11}\, \mathrm{Re}\, Z_{22} \geqslant 0 \quad . \quad . \quad . \quad . \quad . \quad . \quad . \quad . \quad (17)$$

Also, Z_{11} and Z_{22} are positive and real, so that circuits 3 and 4 are absolutely stable in the s-plane region of interest. In addition, Z_{11} and Z_{22} remain positive for all attainable values of G_1 and G_2 owing to the absence of negative terms in the Z parameters. Thus, we may conclude that gyrator circuits 3 and 4 cannot attain low-frequency unstable modes. A root-locus diagram for circuits 3 and 4 is shown in Table 3. In the case considered, circuits 3 and 4 have identical root-locus diagrams. The above conclusions have been confirmed experimentally.

The above stability analysis is valid in the s-plane region $|s| \ll \omega_c$ because real amplifier gains have been assumed. On using the dominant-pole representation for the amplifier gain, given by eqn. 14, an analysis can be produced for gyrator circuits 3 and 4, which is valid in the s-plane region $|s| \leqslant \omega_m$.

The input impedance $Z_i(s)$ of a 2-port loaded by an arbitrary passive impedance $Z_L(s)$ is

$$Z_i(s) = Z_{11} - \frac{Z_{12}Z_{21}}{Z_{22} + Z_L(s)} \quad . \quad . \quad . \quad . \quad . \quad . \quad (18)$$

For passivity, and therefore absolute stability, $Z_i(s)$ must be a positive real (p.r.) function. The following conditions must then be satisfied:[30]

(*a*) $Z_i(s)$ has no poles with positive real part and any imaginary poles are simple

(*b*) $Z_i(s)$ has no zeros with a positive real part and any imaginary zeros are simple

(*c*) $\mathrm{Re}\, Z_i(j\omega) \geqslant 0$ for all ω.

When only conditions *a* and *b* are satisfied, the input impedance is active, and therefore potentially unstable, since a passive termination can be found which can make the network unstable.[30]

For gyrator circuit 3 (or 4), eqn. 18 and the Zparameters in Table 2 yield

$$Z_i(s) = \frac{R^2}{Z_{11}(s) + Z_L(s)} + \frac{Z_{11}(s)Z_L(s)}{Z_{11}(s) + Z_L(s)} \quad . \quad . \quad (19)$$

The assumptions $R_1 = R_2 = R$ and $G_1 = G_2 = G$ which have been made do not impose any restrictions on the usefulness of the gyrator circuit.

From Table 2 and eqn. 14,

$$Z_{11} = \frac{N(s)}{D(s)} = \frac{R\{s^2 + \omega_c(G_o + 2)s + \omega_c^2(G_o + 1)\}}{s^2 + \omega_c(G_o + 2)s + \frac{1}{2}\omega_c^2(G_0^2 + 2G_o + 2)} \quad (20)$$

Since R and $\omega_c \geqslant 0$ and $G_o \geqslant 0$, the zeros of $N(s)$ and $D(s)$ are in the left-half $s$plane. From eqn. 20,

$$\text{Re } Z_{11}(j\omega) = \frac{R(\omega^4 + B\omega^2 + C)}{|D(j\omega)|^2} \quad . \quad . \quad . \quad . \quad (21)$$

where $B = \frac{1}{2}\omega_c^2(G_o + 2)^2$

$C = \frac{1}{2}\omega_c^4(G_o^2 + 2G_o + 2)(G_o + 1)$

The constants B and C are positive so that,

$$\text{Re } Z_{11}(j\omega) > 0 \text{ for all } \omega \quad . \quad . \quad . \quad . \quad . \quad . \quad . \quad (22)$$

Hence $Z_{11}(s)$ satisfies conditions (a)–(c) and is therefore a p.r. function. In addition, it remains a p.r. function for all attainable values of G_o in the range $0 \leqslant G_o \leqslant G_{o\,max}$, where $G_{o\,max} < \infty$.

It is well known[31] that when $H_a(s)$ and $H_b(s)$ are p.r. functions, then $\{H_a(s) + H_b(s)\}$, $\{1/H_a(s)\}$, and $DH_a(s)$ (D is a positive constant) are also p.r. functions. Consequently,

$$\{Z_{11}(s) + Z_L(s)\}$$
$$1/\{Z_{11}(s) + Z_L(s)\}$$
$$R^2/\{Z_{11}(s) + Z_L(s)\}$$

and $$\{1/Z_{11}(s)\} + \{1/Z_L(s)\} \equiv \frac{Z_{11}(s)Z_L(s)}{Z_{11}(s) + Z_L(s)}$$

are also p.r. functions. Thus $Z_i(s)$ is p.r. and can be realised by the passive network shown in Fig. 10.

In effect, the imperfections of gyrator circuits 3 and 4, due

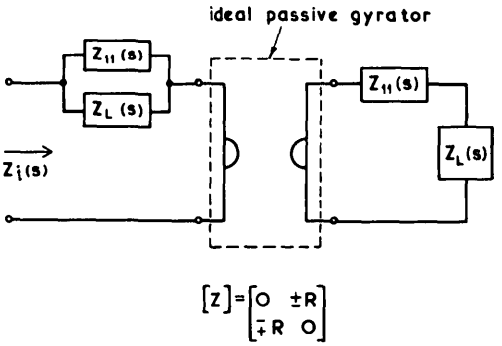

Fig. 10

Equivalent circuit for an imperfect gyrator circuit

to noninfinite and frequency-dependent amplifier gains, introduce series-passive parasitic impedances.

The conclusions of the above analysis can be stated as follows:

Theorem

(i) Gyrator circuit 3 (or 4) having

$$R_1 = R_2 = R$$

$$G_1 = G_2 = \frac{G_o\omega_c}{s + \omega_c}$$

amplifiers with infinite input impedance and zero output impedance, presents a passive input impedance at port 1, when loaded by any passive impedance at port 2.

(ii) The input impedance remains passive for all attainable values of G_o (i.e. $0 \leqslant G_o \leqslant G_{o\,max}$ where $G_{o\,max} < \infty$).

The second part of the above theorem shows that gyrator circuits 3 and 4 do not attain unstable modes just after activation, and so they are unconditionally stable.

7 Experimental results

The parameter ω_c is a function of the compensating elements, and it should be chosen sufficiently small to eliminate high-frequency-unstable modes. However, a small value of ω_c will yield a gyrator circuit with a small bandwidth. In practice, the choice of ω_c depends on the type of amplifier and inversely on the size of G_o.

Some preliminary computer calculations have shown that a finite amplifier input resistance and a nonzero output resistance can produce Qfactor enhancement which may result in negative Qfactors.

The gyrator circuit 4 has been built using amplifiers type 709C. Initial measurements have shown that the Qfactor enhancement is sometimes present, but this can be eliminated by selecting the compensation.

After selecting satisfactory frequency compensations, the Qfactor and gyration constant (k_m) were measured for a nominal gyration constant $k_{nom} = 10^6$ ($k_{nom} = R_1R_2$). The results are shown in Figs. 11*a* and *b*. Polystyrene capacitors were used.

At low frequencies, the deviation in the gyration constant, as shown in Fig. 11*b*, is small and the inductance simulated is relatively independent of amplifier-gain variations. The temperature coefficient of k_m may therefore be prescribed by selecting the temperature coefficients of the gyrator resistors and of the load capacitor. Fig. 11*a* shows that larger Qfactors are feasible in comparison to those encountered in coils.

8 Generalised-impedance convertors

Consider a 2-port network in which the input impedance is a transform of the load impedance, that is

$$Z_i = f(s)Z_L \quad . \quad . \quad . \quad . \quad . \quad . \quad . \quad . \quad . \quad . \quad . \quad (23)$$

Such a network can be defined as a generalised-impedance convertor (g.i.c.) with an impedance-conversion function $f(s)$. Eqn. 23 can be written as

$$\frac{V_1}{I_1} = f(s)\frac{V_2}{(-I_2)} \quad . \quad . \quad . \quad . \quad . \quad . \quad . \quad . \quad . \quad . \quad (24)$$

and can be interpreted as

$$\left.\begin{aligned} V_2 &= \frac{V_1}{f(s)} \\ -I_2 &= I_1 \end{aligned}\right\} \quad . \quad . \quad . \quad . \quad . \quad . \quad . \quad . \quad . \quad . \quad (25)$$

or as

$$\left.\begin{aligned} V_2 &= V_1 \\ -I_2 &= f(s)I_1 \end{aligned}\right\} \quad . \quad . \quad . \quad . \quad . \quad . \quad . \quad . \quad . \quad . \quad (26)$$

Two special types of g.i.c. therefore exist. Eqn. 25 defines a voltage-conversion g.i.c. (v.g.i.c.) and eqn. 26 defines a current-conversion g.i.c. (c.g.i.c.).

The chain matrix of a v.g.i.c. obtained from eqn. 25 is

$$[A]_{v.g.i.c.} = \begin{bmatrix} f(s) & 0 \\ 0 & 1 \end{bmatrix} \quad . \quad . \quad . \quad . \quad . \quad . \quad . \quad . \quad . \quad (27)$$

and similarly from eqn. 26, the chain matrix of a c.g.i.c. is

$$[A]_{c.g.i.c.} = \begin{bmatrix} 1 & 0 \\ 0 & \frac{1}{f(s)} \end{bmatrix} \quad . \quad . \quad . \quad . \quad . \quad . \quad . \quad . \quad (28)$$

The above is, in effect, a simple generalisation of the well known n.i.c. theory. The proposed symbols for a v.g.i.c. and a c.g.i.c. are shown in Figs. 12*a–d* (< for voltage and C for current).

The gyrator circuits 1–4 can be converted into c.g.i.c. circuits by terminating port 2 with an impedance, and removing R_2 to create a new port 2. Gyrator circuits 3 and 4 yield only one c.g.i.c., as shown in Fig. 12*e*. The impedance-conversion function, for ideal infinite-gain amplifiers, is

$$f(s) = \frac{Z_1Z_3}{Z_2Z_4} \quad . \quad . \quad . \quad . \quad . \quad . \quad . \quad . \quad . \quad . \quad . \quad . \quad (29)$$

It is interesting to note that the c.g.i.c. circuit is a 3-terminal 2-port in contrast to the 4-terminal gyrator circuits.

Gyrator circuits will be used as c.g.i.c. circuits for the synthesis of *RC*-active networks in Sections 9 and 10.

Eqn. 29 shows that impedance-conversion functions of the form $k_3 s$, $1/k_3 s$, $k_4 s^2$ and $1/k_4 s^2$ are possible (k_3 and k_4 are positive constants) by using only resistances and capacitances. Also in the particular case when Z_1–Z_4 are resistive, the c.g.i.c. of Fig. 12*e* becomes a current-conversion positive-impedance convertor. This can be used for impedance-matching purposes in the same way as a transformer.

9 Synthesis of *RC*-active networks

RC-active networks (networks comprising resistances, capacitances and amplifiers) can be obtained from passive *RLC* ones by using gyrators to simulate the inductances. In this way, *RC*-active networks can be synthetised whose sensitivity to element variations is comparable to that of passive networks.[4, 32]

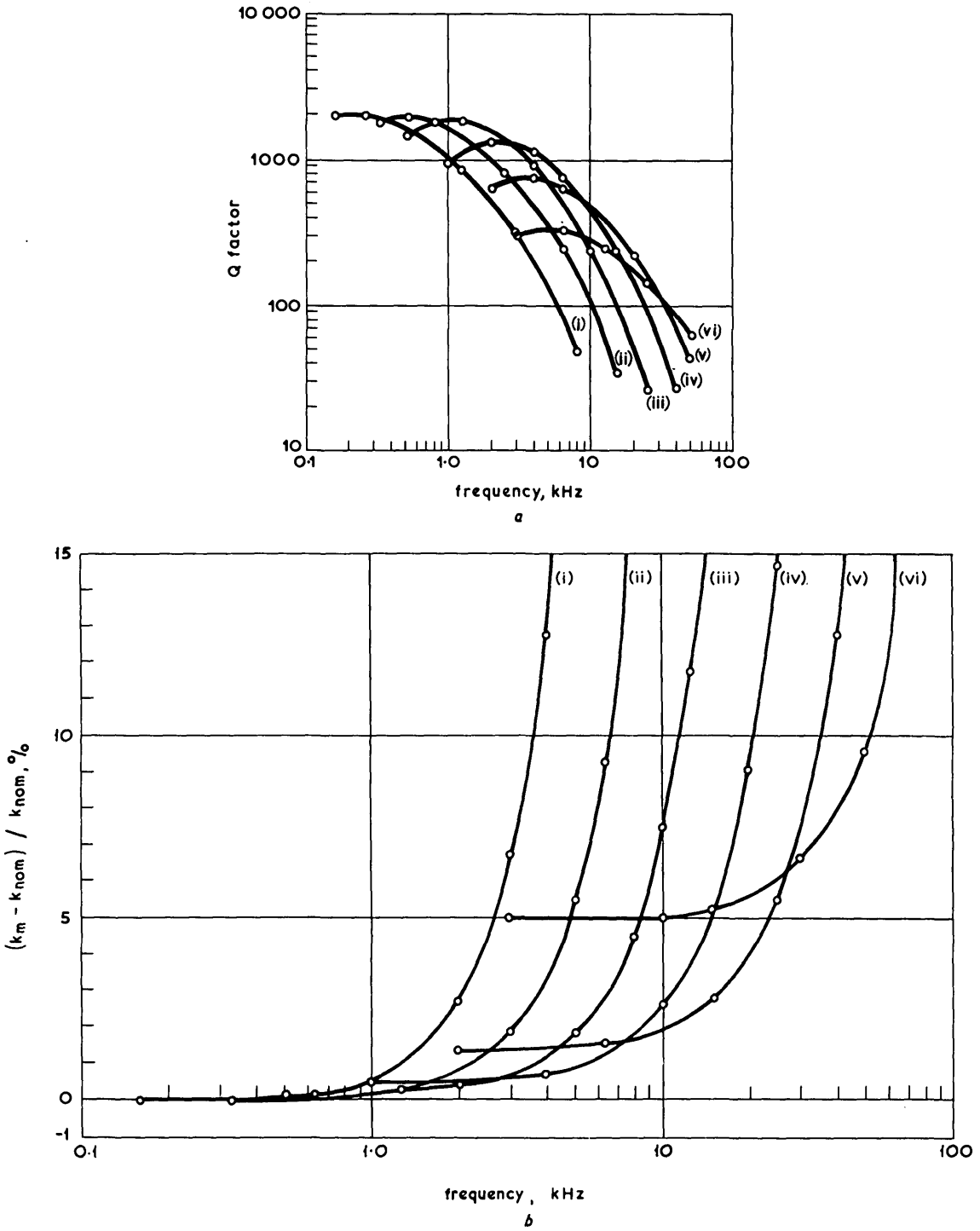

Fig. 11

Experimental results for gyrator 4 having gyration constant $k_n = 10^6$

a Q factor against frequency *b* Gyration-constant deviation against frequency

(i) Load capacitance ≈ 1 μF, inductance = 1 H
(ii) Load capacitance ≈ 0·3 μF, inductance ≈ 0·3 H
(iii) Load capacitance ≈ 0·1 μF, inductance ≈ 0·1 H
(iv) Load capacitance ≈ 0·03 μF, inductance = 0·03 H
(v) Load capacitance ≈ 0·01 μF, inductance = 0·01 H
(vi) Load capacitance = 0·003 μF, inductance ≈ 0·003 H
alternating voltage across inductor ≈ 100 mV
For amplifier—frequency compensation, C_1 ≈ 2000 pF, R_1 1·5 kΩ
C_2 ≈ 39 pF

The gyrator circuits described in Section 5 have one of their input terminals connected permanently to the common terminal of the power supply. Since all the gyrator circuits in a practical network must share a single common-earthed power supply, only grounded inductances are readily obtainable. Although grounded inductances are sufficient to realise high-pass and some bandpass filters,[33] in general, floating inductances are essential.

Sheahan,[34] Holt and Taylor,[35] Riordan[10] and Gorski-Popiel[36] have described methods for obtaining floating inductances. The method proposed by Holt and Taylor is applicable to 3-terminal gyrator circuits but the present

circuits are 4-terminal. The methods of Riordan and Gorski-Popiel use gyrator circuits as g.i.c.s, and, in effect, Gorski-Popiel's method is an interesting generalisation of that of Riordan. Gorski-Popiel's approach leads to a reduction of the number of amplifiers needed, and will be used in the synthesis of active filters; this will now be described.

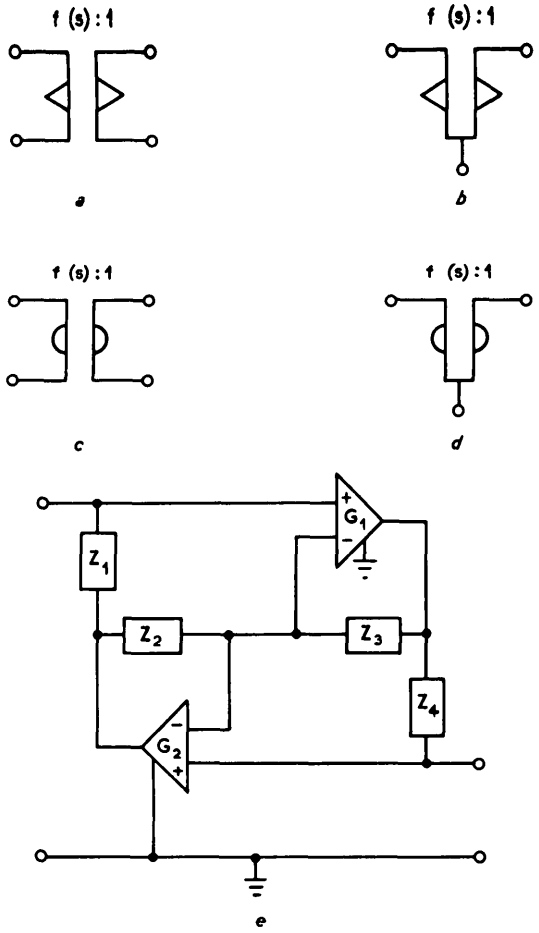

Fig. 12

Generalised-impedance convertors

a and *b* Symbols for 4-terminal and 3-terminal v.g.i.c.
c and *d* Symbols for 4-terminal and 3-terminal c.g.i.c.
(a resistance of 1 Ω across port 2 causes an input impedance $f(s)$; hence the notation $f(s)$:1)
e Practical c.g.i.c. circuit derived from gyrator circuit of Fig. 9*c* (or *d*)

Consider an $(n + 1)$-terminal network N^A, with n g.i.c.s connected as shown in Fig. 13. The Z matrix of N^A is given by

$$[V^A] = [Z^A][I^A] \quad . \quad . \quad . \quad . \quad . \quad . \quad . \quad . \quad . \quad . \quad (30)$$

where $[V^A]$ and $[I^A]$ are voltage and current vectors. Using identical c.g.i.c.s from eqn. 26, $V_1^A = V_1^B$, $V_2^A = V_2^B$, . . . , i.e.,

$$[V^A] = [V^B] \quad . \quad . \quad . \quad . \quad . \quad . \quad . \quad . \quad . \quad . \quad (31)$$

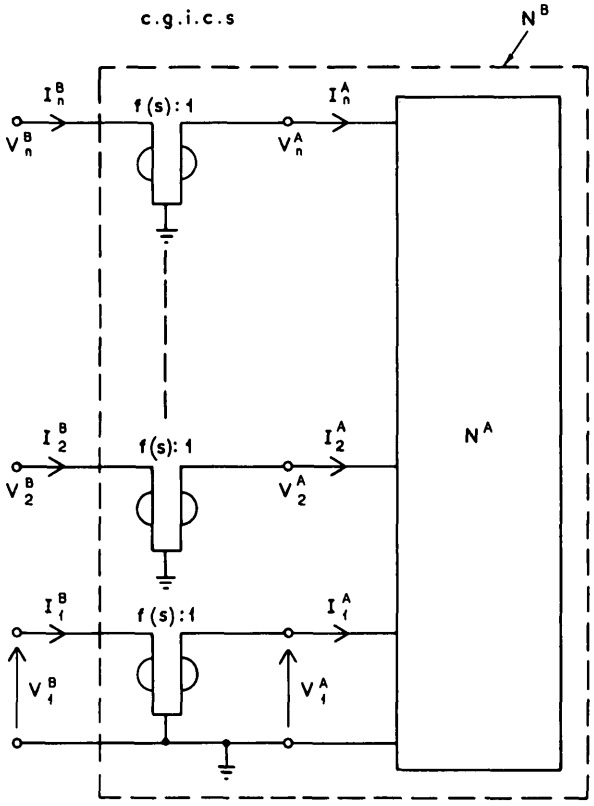

Fig. 13

Realisation of inductive subnetworks

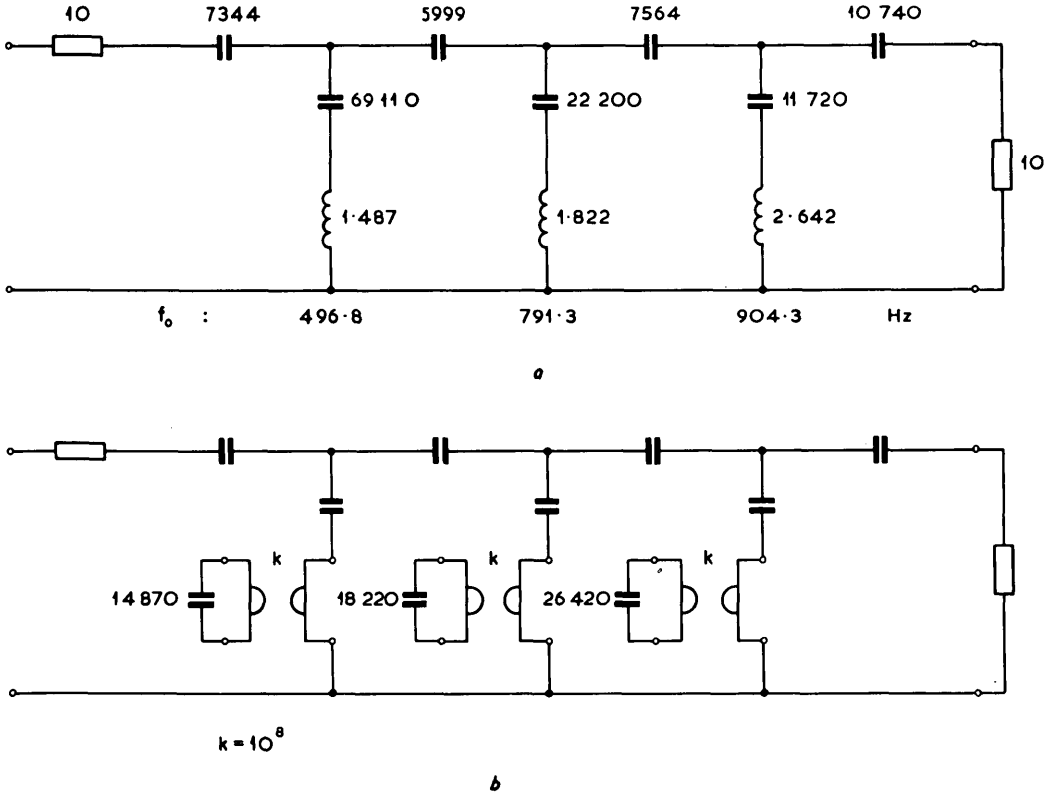

Fig. 14

Highpass filter

a *RLC*-passive realisation
b *RC*-active realisation
(Inductances in henrys, capacitances in picofarads, resistances in kilohms: gyration constant $k = 10^3$)

Similarly $I_1^A = f(s)I_1^B$, $I_2^A = f(s)I_2^B$, . . . , i.e.

$$[I^A] = f(s)[I^B] \quad . \quad . \quad . \quad . \quad . \quad . \quad . \quad . \quad . \quad . \quad (32)$$

From eqns. 30–32,

$$[V^B] = f(s)[Z^A][I^B] = [Z^B][I^B] \quad . \quad . \quad . \quad . \quad . \quad (33)$$

Hence network N^B has

$$[Z^B] = f(s)[Z^A] \quad . \quad . \quad . \quad . \quad . \quad . \quad . \quad . \quad . \quad (34)$$

It is evident that N^B and N^A have the same topology and that each element of N^A is transformed by $f(s)$.

If a resistive N^A and a c.g.i.c. in which $Z_1 = Z_2$ (or Z_4) = $Z_3 = R$ and Z_4 (or Z_2) $= 1/sC$ [i.e. $f(s) = sRC$] are used, the resulting network N^B is inductive. The configuration in Fig. 13 can then be used to realise each connected inductive subnetwork in a passive *RLC* network, yielding an *RC*-active network.

10 Design of highpass and bandpass filters

10.1 Highpass filter

The gyrator circuit in Fig. 9*d* has been used in the realisation of a highpass filter with a maximum passband attenuation of 1·0dB, a minimum stopband attenuation of 60·0dB, a cutoff frequency of 1091 Hz, and a selectivity factor[37] of 0·84. An approximation satisfying these specifications is the elliptic transfer function

$$T(s) = \frac{s}{(s + 3{\cdot}9480)} \times \frac{(s^2 + 0{\cdot}2465)}{(s^2 + 1{\cdot}2208s + 3{\cdot}2701)} \times \frac{(s^2 + 0{\cdot}6261)}{(s^2 + 0{\cdot}2550s + 1{\cdot}5072)} \times \frac{(s^2 + 0{\cdot}8178)}{(s^2 + 0{\cdot}05221s + 1{\cdot}1933)} \quad . \quad . \quad . \quad . \quad (35)$$

A passive *RLC* realisation of this transfer function, obtained by using Skwirzynski's design tables,[37] is shown in Fig. 14*a*.

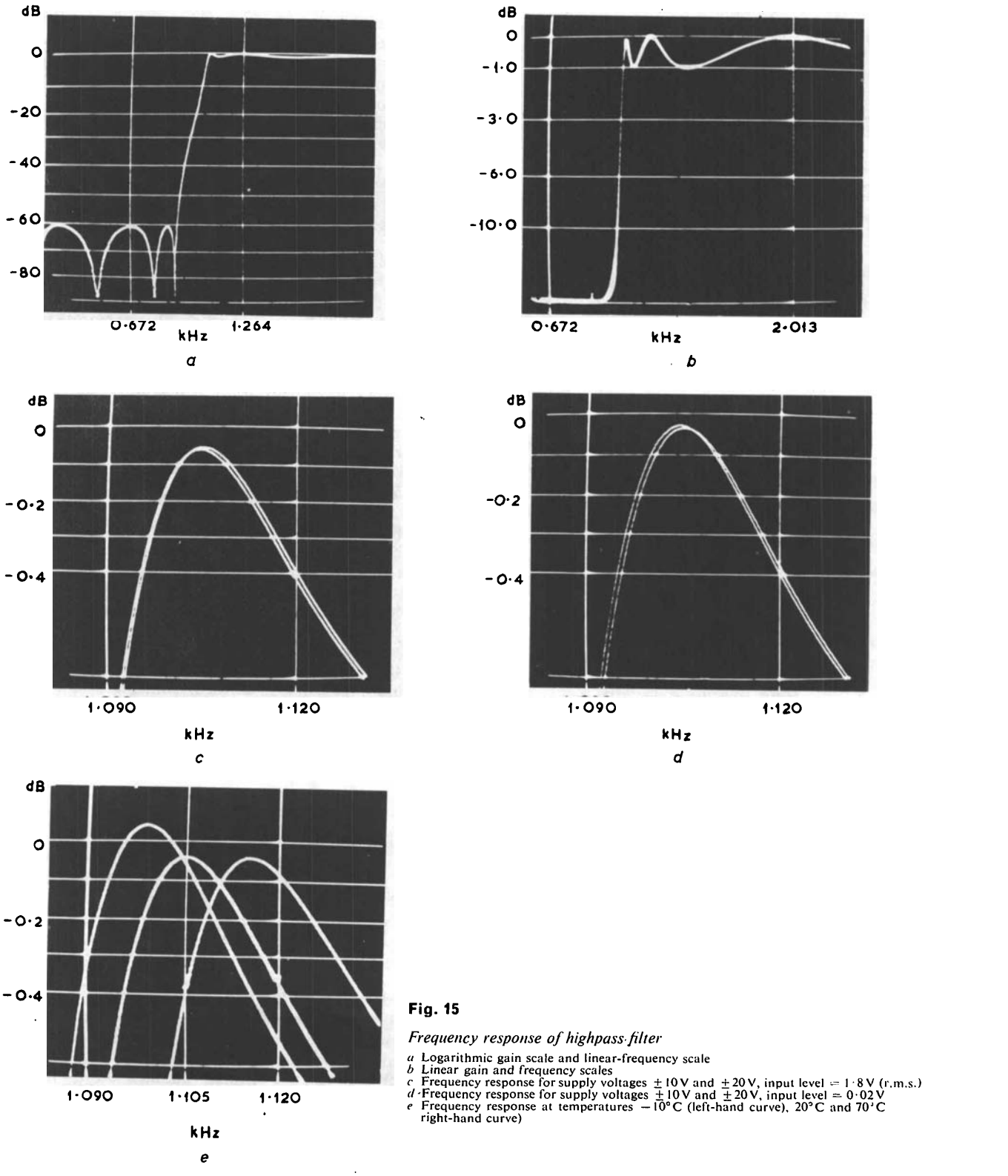

Fig. 15

Frequency response of highpass filter

a Logarithmic gain scale and linear-frequency scale
b Linear gain and frequency scales
c Frequency response for supply voltages ±10V and ±20V, input level = 1·8V (r.m.s.)
d Frequency response for supply voltages ±10V and ±20V, input level = 0·02V
e Frequency response at temperatures −10°C (left-hand curve), 20°C and 70°C right-hand curve)

By replacing each inductance by a gyrator terminated by a capacitance, Fig. 14*b* results. The gyrator circuits were constructed using 10kΩ tin-oxide resistors (gyration constant $k = 10^8$) and μA741C operational amplifiers. The filter was built

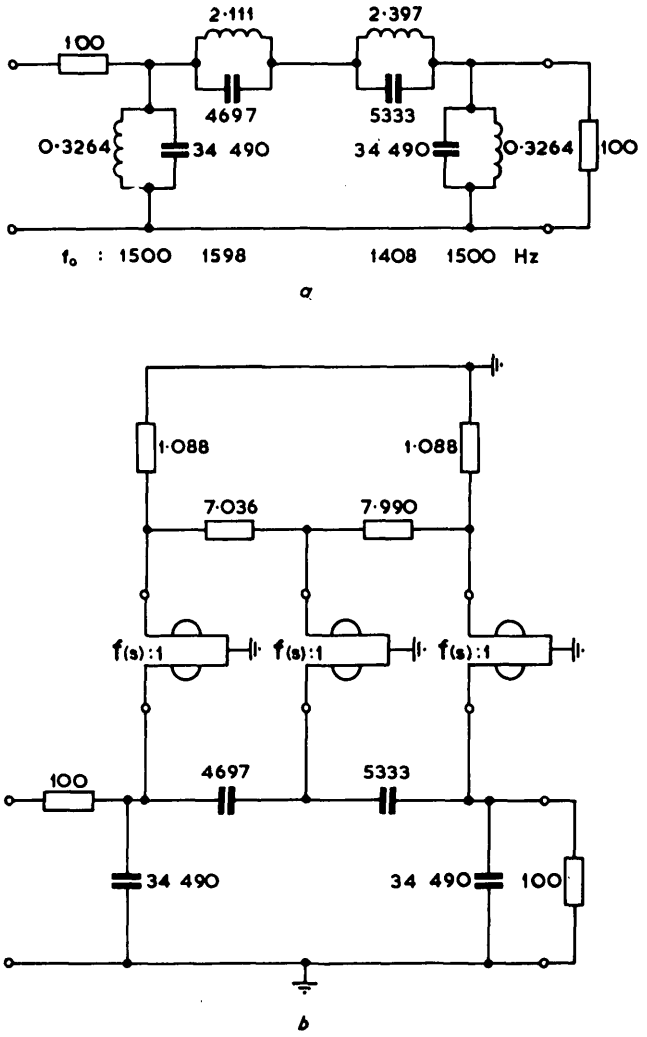

Fig. 16

Bandpass filter

a *RLC*-passive realisation
b *RC*-active realisation
(*L*'s in H, *C*'s in pF, *R*'s in kΩ, $f(s) = 3 \times 10^{-4}s$)

using polystyrene capacitors (temperature coefficient = − 140 ± 40p.p.m./°C, tolerance < 1%) and tin-oxide resistors (temperature coefficient = ± 200p.p.m./°C, tolerance < 1%) and was aligned by adjusting the gyration constants.

The measured frequency response, shown in Figs. 15*a* and *b*, agrees with the theoretical response. The effect of input level and d.c.-supply variations is illustrated in Figs. 15*c* and *d* Each figure shows the frequency response (the frequency and gain scales are centred on the leading ripple) for supply voltages of ±10V and ±20V. In Figs. 15*c* and *d* the input levels are 1·8V (r.m.s.) and 0·02V respectively. The deviation in the passband ripple is about 0·01dB and is, therefore, negligible. The effect of temperature variations is illustrated in Fig. 15*e* which shows the frequency response at −10°C (left-hand curve), 20°C and 70°C (right-hand curve). The leading peak has been displaced horizontally by 15·7Hz which corresponds to a change of 177p.p.m. per deg C. The frequency displacement is due to passive-element variations, and is within the predicted value.

10.2 Bandpass filter

The method described in Section 8 and the c.g.i.c. of Fig. 12*e* have been used for the realisation of a bandpass filter with a maximum passband attenuation of 0·3dB, a minimum stopband attenuation of 38dB, a centre frequency of 1500Hz, and a bandwidth of 60Hz. A suitable approximation is the elliptic transfer function,

$$T(s) = \frac{0{\cdot}003977s}{s^2 + 0{\cdot}03080s + 1} \times \frac{(s^2 + 0{\cdot}8818)}{(s^2 + 0{\cdot}01312s + 0{\cdot}9577)} \times \frac{(s^2 + 1{\cdot}1341)}{(s^2 + 0{\cdot}01370s + 1{\cdot}0442)} \quad (36)$$

A passive *RLC* realisation of the above transfer function, obtained from Reference 37, is shown in Fig. 16*a*. On replacing the inductive subnetwork by the circuit in Fig. 13, the circuit in Fig. 16*b* results. The c.g.i.c.s were built using 10kΩ metal-film resistors (temperature coefficient = ± 100p.p.m./°C, tolerance < 1%) for Z_1, Z_2 and Z_3 and 0·03μF polystyrene capacitors for Z_4. Amplifiers of the type μA 741C were used throughout. The filter was built using tin-oxide resistors and polystyrene capacitors and was aligned by trimming the resistors of network N^A.

The measured frequency response is in agreement with the theoretical response as shown in Figs. 17*a* and *b*. Figs. 17*c* and *d* show the frequency response for supply voltages of ±10V (left-hand curve), ±15V and ±20V (right-hand curve). In Fig. 17*c* the input voltage is 2V and in Fig. 17*d* it is 0·05V. The passband ripple remains less than 0·4dB and the deviation in the stopband is negligible. The effect of temperature variations is similar to that encountered in the highpass filter. The passband ripple remains less than 0·4dB in the temperature range −10–70°C. A centre-frequency displacement of 17Hz has been measured which corresponds to a change of 142p.p.m. per deg C. The bandpass filter has a smaller temperature coefficient than the highpass filter (142 compared to 177) because the c.g.i.c.s incorporate metal-film resistors but the gyrators incorporate tin-oxide ones. It is expected that filters with a very small temperature coefficient can be constructed by selecting a temperature coefficient of the resistors equal and opposite to that of the capacitors.

In conclusion, highpass and bandpass filters have been found to be relatively insensitive to temperature and supply-voltage variations and they remain relatively linear for different input levels.

The operational amplifiers used have fixed internal frequency compensation. In general, however, external compensation is preferable since it can be chosen to optimise the gyrator bandwidth.

In each of the above filters, six amplifiers are needed. If, however, the synthesis procedures in Reference 38 are used, the highpass and bandpass filters require four and three amplifiers, respectively. However, the sensitivity is increased, and, in effect, the bandpass-filter realisation is impracticable since, owing to the high *Q* factors (> 70), very-close-tolerance elements are needed. For stringent specifications and high *Q* factors, the present procedures are preferable, but for undemanding specifications and for *Q* factors less than 20 or 30, the procedures in Reference 38 should be used, since fewer amplifiers are needed.

11 Alternative gyrator circuits

It has been shown in Reference 39 that Riordan's gyrator circuits[10] suffer from the same disadvantage as the gyrator circuits given in Figs. 9*a* and *b*, i.e. they are conditionally stable. By using the theory of singular elements in Riordan's circuits, alternative gyrator circuits have been derived in Reference 39 and these have been shown to be unconditionally stable. In effect, the derived gyrator circuits are similar to those given in Figs. 9*c* and *d*.

The gyrator circuits of the present paper, those of Reference 39 and those of Riordan are 4-terminal 2-ports. In some cases 3-terminal gyrator circuits are needed. Such circuits have been described in Reference 40. The operation of the 3-terminal gyrator circuits depends on the exact cancellation of a negative resistance by a positive resistance, in contrast to the 4-terminal gyrator circuits. Because of this, the 3-terminal circuits are more sensitive to resistance variations than the 4-terminal circuits.

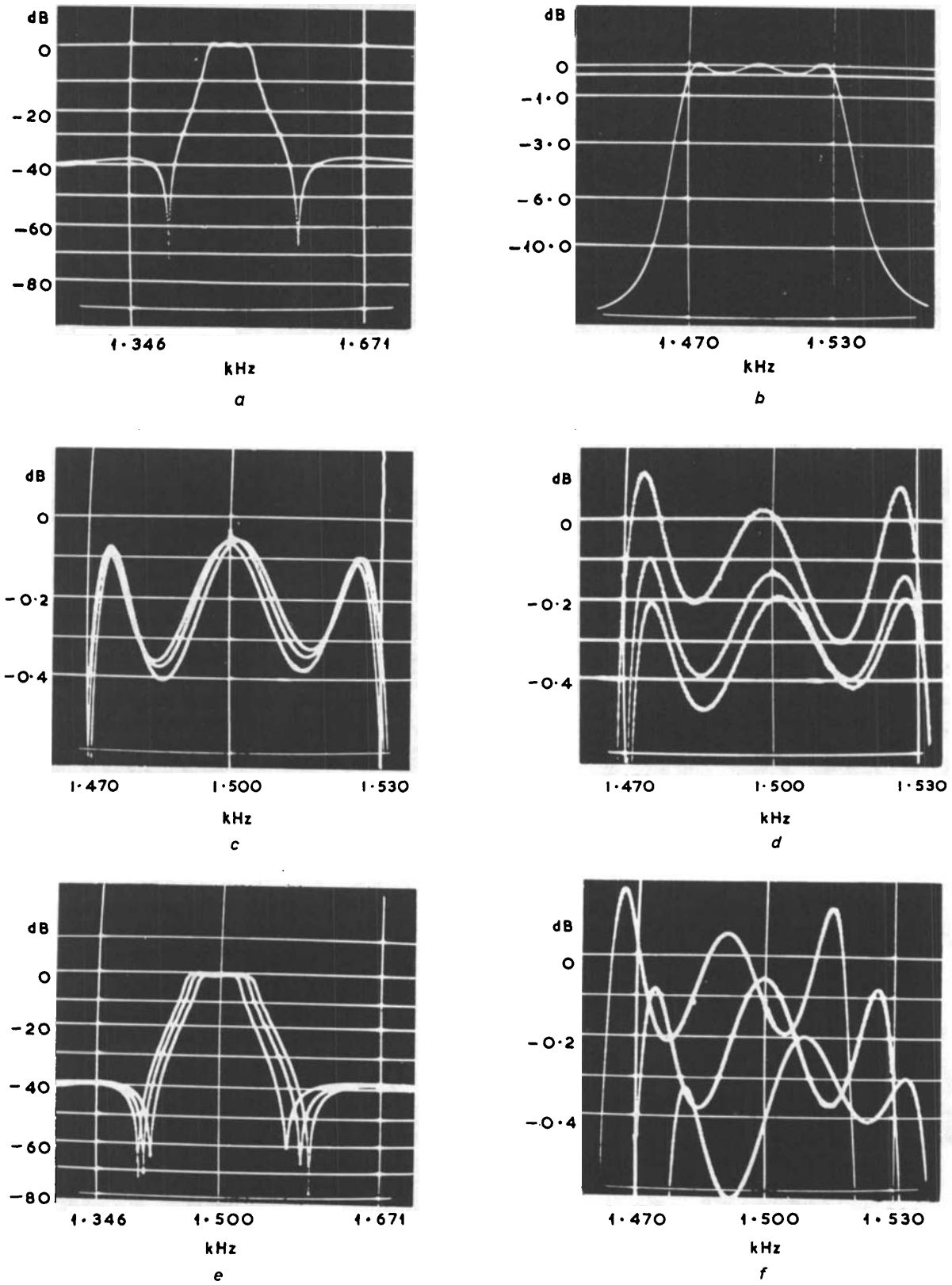

Fig. 17

Frequency response of bandpass filter

a Logarithmic gain scale and linear frequency scale
b Linear gain and frequency scales
c Frequency response for supply voltage of ±10V (left-hand curve) ±15V and ±20V (right-hand curve), input level of 2V
d Frequency response for supply voltage of ±10V (left-hand curve), ±15V and ±20V (right-hand curve), input level of 0·05V
e and *f* Frequency response at temperatures of −10°C (left-hand curve), 20°C and 70°C (right-hand curve)

12 Conclusions

The concept of the singular elements has been found to be very useful in the realisation of gyrators. Two conditionally stable and two unconditionally stable gyrator circuits have been described, but, in practice, the two unconditionally stable circuits should be used. At low frequencies, these circuits have a gyration constant which is insensitive to amplifier gain variations, and the feasible Q factors are larger than those encountered in coils. Consequently, filters with grounded inductors and a low sensitivity to the amplifier gains can be built. This has been illustrated by the highpass-filter design. The gyrator circuits described can be treated as g.i.c.s, which are used for the simulation of floating inductances. The bandpass filter using g.i.c.s has been found to be relatively insensitive to temperature and supply-voltage variations.

13 Acknowledgments

Acknowledgment is made to the Director of Research, Post Office Research Department, for his permission to

publish the information contained in this paper. Thanks are due to J. M. Rollett for his comments, also to D. R. Wise for carrying out the computer programming and building and testing the filters, and to A. J. Greaves for building and testing the gyrator circuits.

14 References

1 RAND, A.: 'Inductor size vs Q: A dimensional analysis', *IEEE Trans.*, 1963, **CP-10**, pp. 31–35
2 ANTONIOU, A.: 'New *RC*-active-network synthesis procedures using negative-impedance convertors', *Proc. IEE*, 1967, **114**, (7), pp. 894–901
3 TELLEGEN, B. D. H.: 'The gyrator, a new electronic network element', *Philips Res. Rep.*, 1948, **3**, pp. 81–101
4 ORCHARD, H. J.: 'Inductorless Filters', *Electron. Lett.*, 1966, **2**, pp. 224–225
5 MORSE, A. S., and HUELSMAN, L. P.: 'A gyrator realisation using operational amplifiers', *IEEE Trans.*, 1964, **CT-11**, pp. 277–278
6 SHENOI, B. A.: 'Practical realisation of a gyrator circuit and *RC*-gyrator filters', *ibid.*, 1965, **CT-12**, pp. 374–380
7 RAO, T. N., and NEWCOMB, R. W.: 'Direct-coupled gyrator suitable for integrated circuits and time variation', *Electron. Lett.*, 1966, **2**, pp. 250–251
8 CHUA, H. T., and NEWCOMB, R. W.: 'Integrated direct-coupled gyrator', *ibid.*, 1967, **3**, pp. 182–184
9 SHEAHAN, D. F., and ORCHARD, H. J.: 'Integratable gyrator using m.o.s. and bipolar transistors', *ibid.*, 1966, **2**, pp. 390–391
10 RIORDAN, R. H. S.: 'Simulated inductors using differential amplifiers', *ibid.*, 1967, **3**, pp. 50–51
11 YANAGISAWA, T., and KAWASHIMA, Y.: 'Active gyrator', *ibid.*, 1967, **3**, pp. 105–107
12 SHARPE, G. E.: 'The pentode gyrator', *IRE Trans.*, 1957, **CT-4**, pp. 321–323
13 GHAUSI, M. S., and MCCARTHY, F. D.: 'A realisation of transistor gyrators', *Solid State Technol.*, 1964, **7**, pp. 13–17
14 PRESCOT, A. J.: 'Loss-compensated active gyrator using differential-input operational amplifiers', *Electron. Lett.*, 1966, **2**, pp. 283–284
15 LARKY, A. I.: 'Negative-impedance converters', *IRE Trans.*, 1957, **CT-4**, pp. 124–131
16 LUNDRY, W. R.: 'Negative impedance circuits—some basic relations and limitations', *ibid.*, 1957, **CT-4**, pp. 132–139
17 CARLIN, H. J., and YOULA, D. C.: 'Network synthesis with negative resistors', *Proc. Inst. Radio Engrs.*, 1961, **49**, pp. 907–920
18 CARLIN, H. J.: 'Singular network elements', *IEEE Trans.*, 1964, **CT-11**, pp. 67–72
19 MARTINELLI, G.: 'On the nullor', *Proc. Inst. Elect. Electron. Engrs.*, 1965, **53**, p. 332
20 BUTLER, E.: 'The operational amplifier as a network element'. Systems Theory Group technical report 86, Cornell University, USA
21 DAVIES, A. C.: 'The significance of nullators, norators and nullors in active-network theory', *Radio Electron. Engr.*, 1967, **34**, pp. 259–267
22 TELLEGEN, B. D. H.: 'On nullators and norators', *IEEE Trans.*, 1966, **CT-13**, pp. 466–469
23 BRAUN, J.: 'Equivalent n.i.c. networks with nullators and norators', *ibid.*, 1965, **CT-12**, pp. 411–412
24 MORSE, A. S.: 'The use of operational amplifiers in active network theory', *Proc. Nat. Electron. Conf.*, 1964, **20**, pp. 748–752
25 ANTONIOU, A.: 'Gyrators using operational amplifiers', *Electron. Lett.*, 1967, **3**, pp. 350–352
26 BROWNLIE, J. D.: 'On the stability properties of a negative-impedance converter', *IEEE Trans.*, 1966, **CT-13**, pp. 98–99
27 ANTONIOU, A.: 'New gyrator circuits obtained by using nullors', *Electron. Lett.*, 1968, **4**, pp. 87–88
28 BODE, H. W.: 'Network analysis and feedback amplifier design' (Van Nostrand, 1945)
29 LLEWELLYN, F. B.: 'Some fundamental properties of transmission systems', *Proc. Inst. Radio Engrs.*, 1952, **40**, pp. 271–283
30 DEPIAN, L.: 'Linear active network theory' (Prentice-Hall International, 1962)
31 HAZONY, D.: 'Elements of network synthesis' (Reinhold, 1963)
32 SHEAHAN, D. F., and ORCHARD, H. J.: 'Bandpass-filter realisation using gyrators', *Electron. Lett.*, 1967, **3**, pp. 40–42
33 'A handbook on electrical filters' (White Electromagnetics Inc., 1963), p. 168
34 SHEAHAN, D. F.: 'Gyrator-flotation circuit', *Electron. Lett.*, 1967, **3**, pp. 39–40
35 HOLT, A. G. J., and TAYLOR, J.: 'Method of replacing ungrounded inductors by grounded gyrators', *ibid.*, 1965, **1**, p. 105
36 GORSKI-POPIEL, J.: '*RC*-active synthesis using positive-immittance convertors', *ibid.*, 1967, **3**, pp. 381–382
37 SKWIRZYNSKI, J. K.: 'Design theory and data for electrical filters' (Van Nostrand, 1965)
38 ANTONIOU, A.: 'Synthesis of active filters with optimum sensitivity', *Radio Electron. Engr.*, 1968, **36**, pp. 135–147
39 ANTONIOU, A.: 'Stability properties of some gyrator circuits', *Electron. Lett.*, 1968, **4**, pp. 510–512
40 ANTONIOU, A.: '3-terminal gyrator circuits using operational amplifiers', *ibid.*, 1968, **4**, pp. 591–592